Propulsion System Instrumentation Development and Integration on Small- and Medium-Sized Electric Unmanned Aircraft

Or D. Dantsker *
Technical University of Munich, Garching, Germany

Renato Mancuso†
Boston University, Boston, MA 02215

With the increasing popularity of unmanned aircraft for both research, military, and commercial applications, significant effort has been undertaken in order to improve these aircraft's performance and flight characteristics. Unmanned aircraft research and development is often based on or culminates with flight testing and significant effort has been undertaken to integrate an increasing amount of sensing into these vehicles. In the end all flight testing efforts depend on the ability to acquire and utilize high fidelity flight data from a large range of sensors and devices. On electrically-propelled unmanned aircraft, collecting propulsion system data is especially vital in determining aircraft state. Broadly, this includes: rotation rate(s) of propellers, fans, or rotors; voltage, current, and temperature at each system component, and energy state of storage components. To collect these measurements, sensors are placed throughout an aircraft with data being sent to a central avionics system, such as a data acquisition system or autopilot. This paper focuses on the requirements, design, development, and integration to perform in-flight measurements of propulsion system parameters on small- and medium-sized electric unmanned aircraft. First, the paper provides an overview for the development of a data acquisition systems on unmanned aircraft followed by the instrumentation aspects involved in integrating propulsion system sensors and interfaces into existing system architectures. Then, the paper presents propulsion system sensing integration examples in 3 different types of electric unmanned aircraft used for research.

Nomenclature

ADC	=	analog-to-digital converters
DOF	=	degree of freedom
ESC	=	electronic speed controller
GPS	=	global positioning system
GNSS	=	global navigation satellite system
IC	=	integrated circuit
IMU	=	inertial measurement unit
I/O	=	input output
MPPT	=	maximum power point tracking
PCB	=	printed circuit board
PWM	=	pulse width modulation
RC	=	radio control
UAV	=	unmanned aerial vehicle

I. Introduction

With the increasing popularity of unmanned aircraft for both research, military, and commercial applications, significant effort has been undertaken in order to improve these aircraft's performance and flight characteristics. Unmanned aircraft research and development is often based on or culminates with flight testing. In just the past several years, along with the uptrend in unmanned aircraft use, there has been an increase in the research related to

*Researcher, Department of Mechanical Engineering, or.dantsker@tum.de
†Assistant Professor, Department of Computer Science. rmancuso@bu.edu

them. Significant effort has been put into studying their aerodynamic qualities,[1–3] especially in high angle-of- attack conditions,[4–6] as well as the development of new control algorithms.[7–12] In addition, unmanned aircraft are often used as low-cost stand-ins for experiments that are too risky or costly to perform on their full scale counterparts.[13–15] They are often also used to explore new aircraft configurations[16–19] or flight hardware.[20–22] In the end, all of these efforts depend on the ability to acquire and utilize high fidelity flight data from a large range of sensors and devices.

On electrically-propelled unmanned aircraft, collecting propulsion system data is especially vital in determining aircraft state. Broadly, this includes: rotation rate(s) of propellers, fans, or rotors; voltage, current, and temperature at each system component, and energy state of storage components. To collect these measurements, sensors are placed throughout an aircraft with data being sent to a central avionics system. The data is centrally collected and distributed and/or logged by a data aggregator, which is likely a data acquisition system or autopilot. However, given that the sensors often monitor high power components, care must be taken in system design, development, and integration in order to minimize danger while acquiring the desired measurements.

This paper focuses on the requirements, design, development, and integration methods employed to perform in-flight measurements of propulsion system parameters on small- and medium-sized electric unmanned aircraft. The paper first provides an overview for the development of a data acquisition systems on unmanned aircraft. Next, it focuses on the instrumentation aspects involved in integrating propulsion system sensors and interfaces into existing system architectures. Then, the paper presents propulsion system sensing integration examples in 3 different types of fixed-wing aircraft: (1) a high-performance aerobatic unmanned aircraft, (2) a small, trainer-type testbed, and (3) an ultra-efficient, long-endurance solar-powered unmanned aircraft. These examples include aircraft specifications, data acquisition system overview and diagrams, and propulsion sensing design, and integration. The paper concludes with a summary.

II. Data Acquisition Overview

The first and likely most critical consideration that must be taken into account is that of the intended uses of a platform and the sensors required. Essentially, what data must be captured and why? On the type of aircraft this paper focuses on, this list would likely include measurements from inertial, global positioning (GPS), analog, actuation (servo PWM), ported air-data, and propulsion sensors (commanded throttle, power, RPM).

The next consideration is that of platform integration, i.e., how will it be integrated into the aircraft and therefore, if there are size, weight, access constraints. This is especially important on small unmanned aircraft, which leads to the notion that a platform must likely be highly integrated; however, at the same time, such tight integration can be restrictive, especially if modifications must be made. Should the platform designer, for example, split the data acquisition between multiple logical devices, sending all of the measurements back into a central device. This could be advantageous in distributing the work, especially if some logical devices can be given the task of handling high-level tasks while others handle low-level tasks. Yet implementing such a platform design may lead to sensory streams having undesirable temporal properties, which in turns affects the quality of produced data. Alternately, the platform be made up of a single logical device prudently managing all of the sensors and measurement devices. Generally, performing benchmark testing of a platform will help determine which approach should be used.

In order to reach design maturity, testing is key. Initial development is often performed by piecing together and interconnecting a set of mostly independent, integrated circuit (IC) components, each on their own printed circuit board (PCB). The strict segregation of components is initially used to test each and every subsystem individually, while designing the software/hardware infrastructure with the integration goal in mind. The *divide et impera* approach has shown to produce highly reliable sensor-processor communication. Then, as the system is miniaturized, these components moved into close proximity with each other. Apart from the obvious hardware integration, subtle signal interplay and similar issues arising from circuit-level integration must be extensively investigated and addressed. Many issues are largely software dependent, as timing properties of software-hardware interaction routines need to be re-calibrated once all the subsystems are contemporarily active. For other issues, new revision of the hardware layout are often required and yield the most reliable solution in terms of reliability and robustness. Flight testing, throughout the whole miniaturization process also reveals several other challenges that cannot be discovered on the ground. These challenges along with the methods used to overcome them will be highlighted.

Minimizing the time required to develop and integrate a platform into an aircraft is also very important and thus a crucial design driver that must be taken into account. Effectively, there is little point to perform system development if the end results will either be too late to meet a project timeline or be impossible to integrate. Therefore, significant effort should be put into developing a self-contained system that could be assembled, installed, and controlled. Regarding control, the end use researcher must be able to interface with the platform in order to communicate required commands. This can mean a wired or wireless connection; however, extra care should be taken with the latter for some applications, especially those with possible RF interference. Thus, the goal of this particular design effort is to ensure that in a complex environment, as most aircraft testing setups are, the platform can be self-contained, not cause interference, and finally be controllable. Effectively, this describes the deployability of the platform solution, which is especially difficult on small electric unmanned aircraft. Further discussion of data acquisition system development and integration can be found in previous work.[23]

III. Propulsion System Instrumentation

Propulsion system instrumentation can be broken down into input and output sensing. More specifically, for input sensing refers to instrumenting the elements that provide power within the propulsion system, i.e. batteries, fuel cells, solar arrays, and (solar) charge controllers. Meanwhile, output sensing refers to instrumenting elements that consume power within the propulsion system, i.e. motor electronic speed controller (ESC), motors and propellers. As all of these components are linked, power balance equations may be formulated to analyze the propulsion system of an aircraft. For example, an integrated power model was developed for electric and solar-powered unmanned aircraft in related work.[24]

Generally, input sensing consists of direct power measurements of voltage and current. Voltage measurements may be direct or, if the potential exceeds the limitations of the input, may use a voltage divider circuit to reduce the output voltage by a fraction. Voltage measurements are typically performed using analog-to-digital converters (ADCs); an example ADC is shown in Figure 1. Current measurements can be in-line as in the case of a shunt resistor current sensor or external as in the case of a hall effect current sensor. It should be mentioned that using a shunt resistor may create relatively significant power losses through the resistor if high current are measured. Examples of current sensors are shown in Figures 2 and 3. Current sensors typically produce measurements in the form of voltage, which is then measured by an ADC; meanwhile, some may output measurements over a communication interface such as UART or I2C. Voltage and current sensors are often isolated from the logical avionics systems using opto-isolators (also called optocouplers) to prevent a potential flow of current that might damage the avionics from the high-power propulsion system components.

Output sensing on the other hand may consist of both direct power measurements of voltage and current as well as indirect power measurements of motion. Direct power measurements are performed using the same voltage and current sensors as described above. Meanwhile, indirect power measurements are performed by measuring the motion of the aircraft and its components. Specifically, an example of this is measuring the power output of a motor based on performance and efficiency knowledge of the motor and propeller, measurement of the propeller rotation rate, and measurement of aircraft freestream velocity. For this example, motor performance and efficiency can be calculated using a first order analytical model[25] and specifications found in the motor datasheet. Propeller performance and efficiency (CT, CP, η vs. J curves) can be derived using blade element momentum theory (BEMT) and sectional airfoil theory as done in[26] or can be obtained experimentally from wind tunnel propeller testing and/or an existing databases.[27,28] Rotation rate is then measured using a tachometer, which can be optical, magnetic, or pulse-based; several examples are shown in Figure 4. Finally, aircraft freestream velocity can be measured using a pitot probe. Indirect propulsion system output measurements is common on unmanned aircraft, especially in post-flight analysis.[29,30] A similar indirect method using torque and thrust measurement to calculate shaft and propeller power is common place in wind tunnel testing.[31–34]

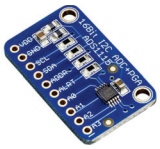

Figure 1. Analog-to-digital converter (ADC) breakout board (photos taken from Adafruit[35]).

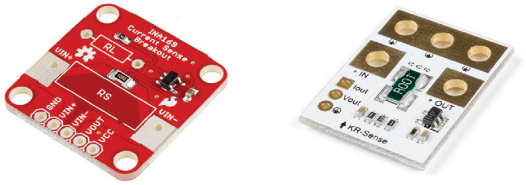

(a) (b)

Figure 2. Shunt resistor current sensor examples: (a) a low-current sensor on a breakout board and (b) a high-current sensor on a sensor board (photos taken from Sparkfun[36]).

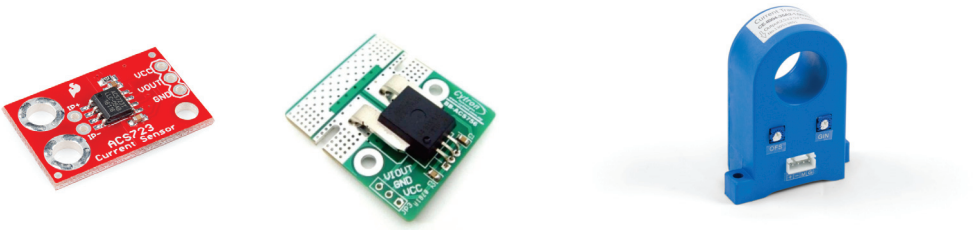

(a) (b) (c)

Figure 3. Hall effect current sensor examples: (a) a low-current integrated Hall-effect current sensor on a breakout board (photo taken from Sparkfun[36]), (b) a high-current integrated Hall-effect current sensor on a sensor board (photo taken from Cytron[37]), and (c) an open-loop Hall-effect current sensor (photo taken from Phidgets[38]).

(a) (b) (c)

Figure 4. Tachometer examples: (a) an optical tachometer, (b) a magnetic tachometer, and (c) a motor ESC with a built-in motor pulse tachometer and output capabilities (photo taken from Castle Creations[39]).

IV. Application Examples

In order illustrate the integration of a propulsion system instrumentation into unmanned aircraft, we look at several integration cases that the authors performed in previous works. The example aircraft are (1) the high-performance, aerobatic UIUC Subscale Sukhoi,[6] (2) the small, trainer-type UIUC Avistar UAV testbed,[40–42] and (3) the ultra-efficient, long-endurance solar-powered UIUC-TUM Solar Flyer .[43–45] These three aircraft are shown in Figure 5 and are distinctly different types of aircraft with different types of development and integration challenges. Two data acquisition systems, the UIUC SDAC[46,47] and the Al Volo FC+DAQ[48] were used on these aircraft; the systems are shown in Fig. 6.

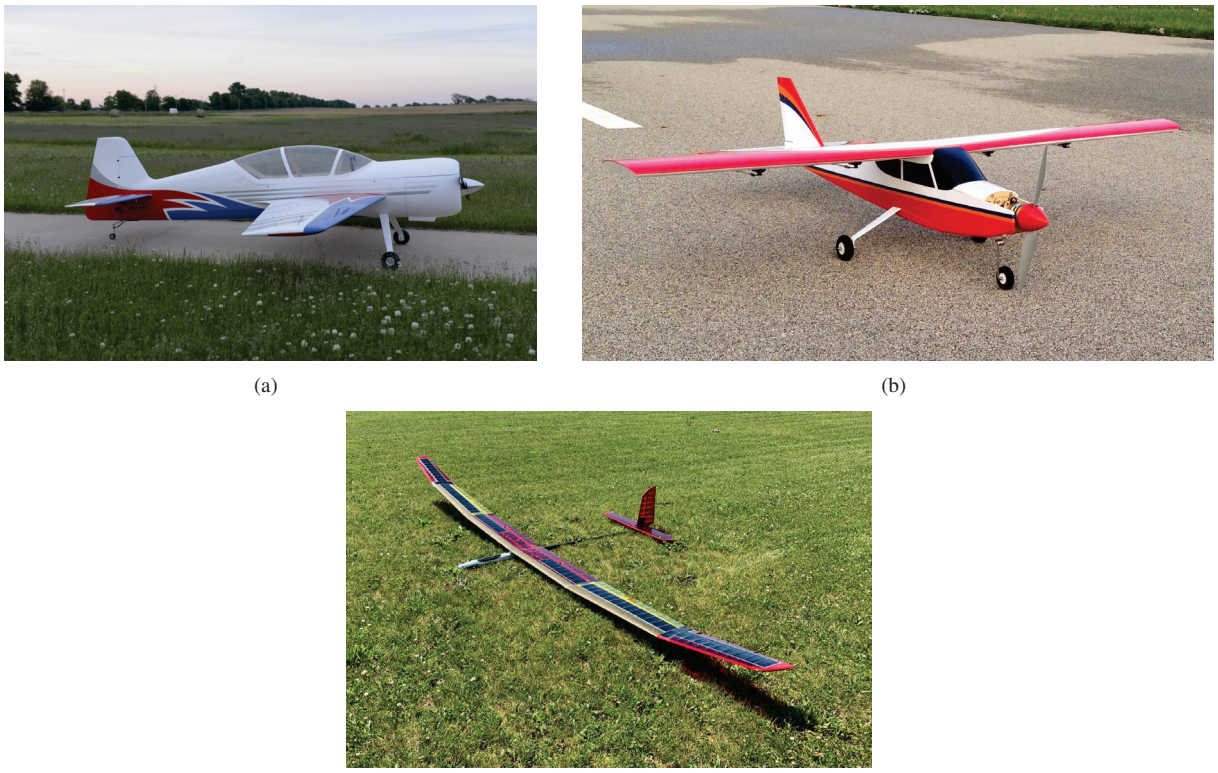

(a) (b)

(c)

Figure 5. Aircraft used as examples: (a) UIUC Subscale Sukhoi, (b) UIUC Avistar UAV, and (c) UIUC-TUM Solar Flyer.

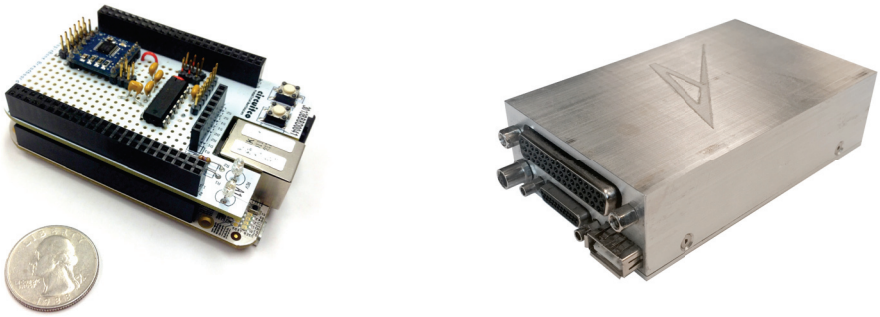

(a) (b)

Figure 6. Data acquisition systems used in the example application: (a) UIUC SDAC and (b) Al Volo FDAQ (photo taken from Al Volo[48]).

A. UIUC Subscale Sukhoi

The UIUC Subscale Sukhoi was developed to perform aerodynamics research in the full-envelope flight regime, specifically to capture unsteady aerodynamic effects exhibited during high angle-of-attack flight. The unmanned aircraft was built from a 35% scale, 2.6 m (102 in) wingspan Sebart Sukhoi 29S electric radio control (RC) model, which provided a light yet robust structure that along with large control surfaces, that allowed the aircraft to perform aggressive aerobatic maneuvers. The aircraft used an electric propulsion system in place of an internal combustion gasoline engine to provide near constant performance, increased reliability, and low vibrations; a list of propulsion system components is given in Table 1. The aircraft was instrumented with the custom-made UIUC SDAC,[40,46,47] which had been recently developed. A system diagram depicting the specific configuration of the instrumentation, along with the flight control and propulsion systems, is shown in Figure 7; the specifications of the components used are listed in Table 2.

Figure 8 shows a diagram of the propulsion system components and how the sensors integrate into it. Specifically, a voltage divider circuit was used to measure the potential of the high propulsion system voltage; this measurement is performed at *ELECT* Port and connects to an ADC on the SDAC. The propulsion system current, between the batteries and the ESC, is measured using a open-loop Hall-effect sensor, which is shown in Figure 9); the output from the Hall-effect sensor is also connected to the *ELECT* Port and then to an ADC. Finally, a pulse tachometer was connected to the wires between the motor and motor ESC at *RPM* Port to measure the propeller and motor rotation rate. Using the sensors, the input power of the propulsion system, between the batteries and the ESC can be computed directly from the product of the measured voltage and current. The output power of the propulsion system at the propeller and motor can be computed indirectly given the rotation rate and airspeed (measured by the airspeed probe) and knowledge of the motor parameters and propeller performance and efficiency gathered in related work.[49]

Table 1. UIUC Subscale Sukhoi unmanned aircraft propulsion system component specifications

Propulsion	
Motor	Hacker A150-8 Outrunner
ESC	Hacker MasterSPIN 220
Propeller	Mejzlik 27x12TH
Motor Flight Pack	(4) Thunder Power ProPerformance 45c 7S 5000 mAh in 2S2P config.
Motor Power Switch	Emcotec SPS 120/240

Table 2. UIUC SDAC system component specifications as installed on the UIUC Subscale Sukhoi

Processing unit	BeagleBone running 32-bit Ubuntu Linux
Sensors	
IMU	XSens Mti-g 6-DOF IMU with Wi-Sys WS3910 GPS Antenna
Airspeed probe	EagleTree Systems pitot-static probe
Airspeed sensor	All Sensors 20cmH2O-D1-4V-MINI differential pressure sensor
Analog-to-digital converters	4x Gravitech 12 bit - 8 Channel ADC
Potentiometers	BI Technologies 6127
Tachometer	Sparkfun ProMicro
Current sensor	Phidgets open-loop hall effect sensor
Magnetometer	PNI Corp MicroMag3
Power	
Regulators	Castle Creations CCBEC
Batteries	30cmThunder Power ProLite 3S 1350 mAh (avionics, telemetry and/or video)
Telemetry transceiver	Digi 9X Tend 900-MHz card
Data Storage	8GB microSD card

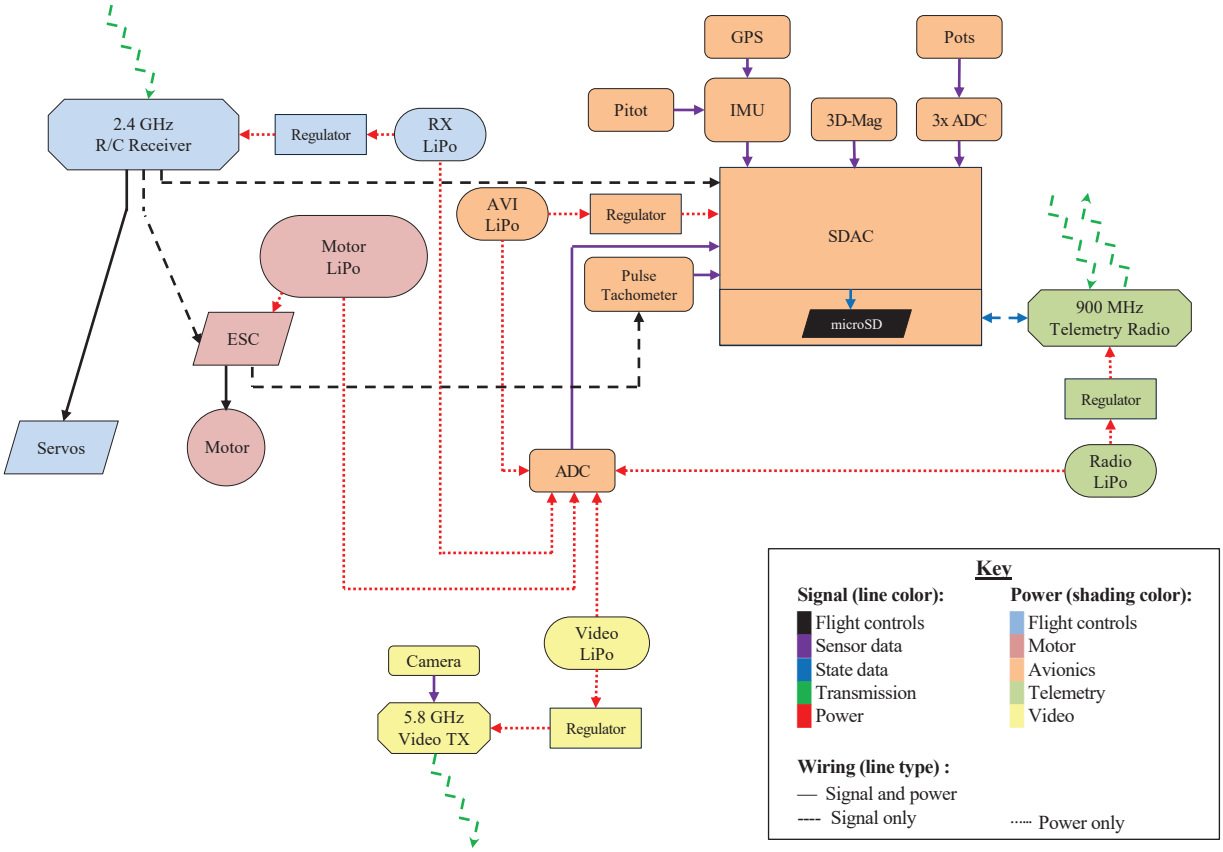

Figure 7. A block diagram of the UIUC SDAC as installed in the UIUC Subscale Sukhoi

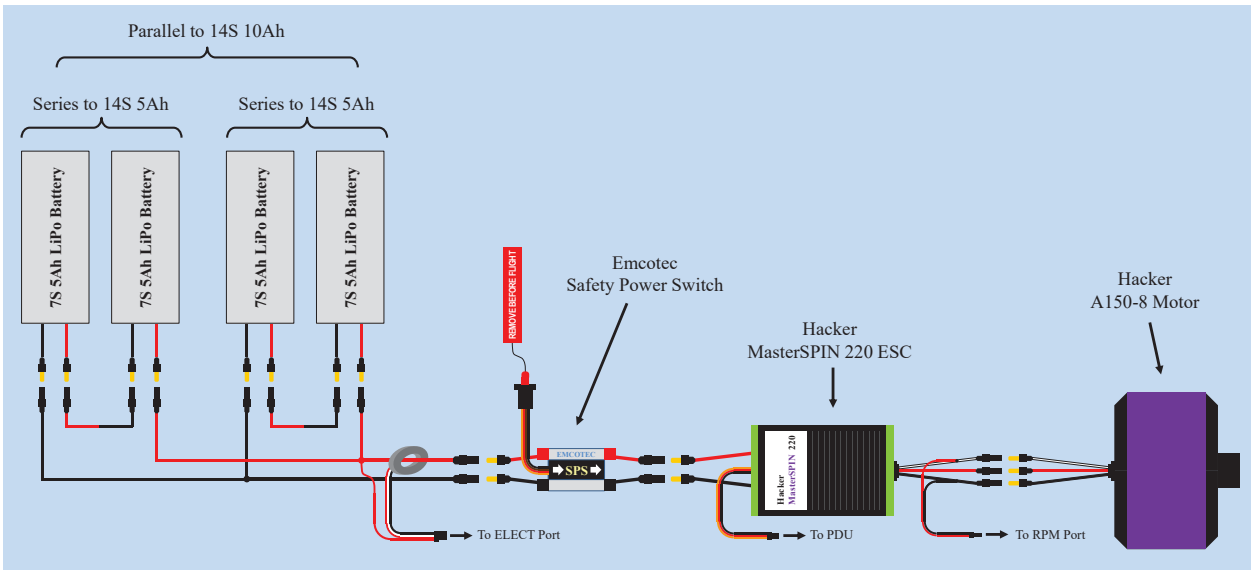

Figure 8. A propulsion system diagram for the UIUC Subscale Sukhoi unmanned aircraft

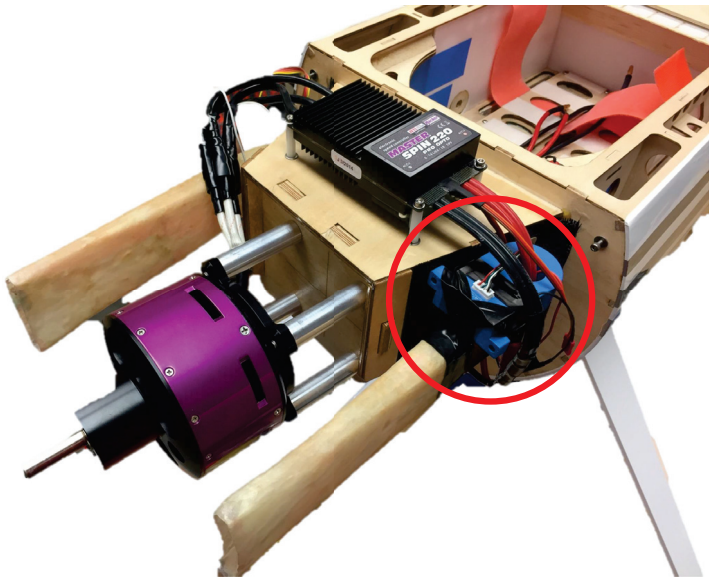

Figure 9. The open-loop Hall-effect current sensor (circled in red) in the UIUC Subscale Sukhoi with the cowling removed; also visible is the propulsion system voltage taps (within the red circle).

B. UIUC Avistar UAV

The Avistar UAV is based on the commercially-available, Great Planes Avistar Elite model airplane trainer, and has been adapted for various research efforts to develop testing methodology, tools, and software.[46,50,51] The aircraft has a wingspan of 1.6 m (62.5 in), a mass of 3.9 kg (8.6 lb), was constructed mainly following manufacturer recommendation with the exception of the propulsion system change and some small improvements to the control surface actuator linkages. The aircraft provided an option of propulsion systems, either a small internal combustion engine or an electric motor; the latter was chosen (similarly to the Subscale Sukhoi) for constant performance, increased reliability, and low vibrations. A list of propulsion system components is given in Table 3. Further testbed details regarding construction, physical, and component specifications can be found in related literature.[52]

The aircraft is instrumented with an Al Volo FC+DAQ[48] flight control and data acquisition system. The system operates at 400 Hz and integrates with a 9 degree-of-freedom (9-DOF) XSens MTi-G-700[53] IMU with a GPS receiver. A pitot-static probe is installed at the tip of the left wing. The pilot commands are also recorded by measuring the pulse width modulation (PWM) signals generated by receiver. Using the sensors, the system is able to log and transmit: 3D linear and angular accelerations, velocities, and position along with GPS location; pitot-static probe airspeed; 3D magnetic field strength and heading; control surface deflections; and propulsion system parameters. The specifications of the avionics used on the UIUC Avistar UAV are listed in Table 4. Further details regarding data acquisition can be found in related literature.[23]

Propulsion system information, including motor voltage, current, rotation rate, and throttle input is logged by FDAQ through an interfaces with the Castle Creations Phoenix Edge 75A ESC used on the aircraft. Additionally, a high-current, integrated Hall-effect sensor was connected between the batteries and ESC to provide system input current measurements; this Hall-effect sensor and the ESC are shown in Figure 10. Using the two current sensors before and in the ESC, the input propulsion power (going from the batteries into the ESC) and the motor propulsion power (going from the ESC into the motor) can be directly computed. Knowledge of these two power values allows one to determine ESC efficiency in-flight; this is a topic that will be explored in future work. Additionally, Similarly to the Subscale Sukhoi, the propulsion system output power can be computed using the propeller rotation rate and the airspeed given knowledge of propeller performance and efficiency.[27] Furthermore, the motor propulsion power (going from the ESC into the motor; measured using the ESC), can be indirectly computed using the analytical motor model; this allows for assessment of ESC current measurement accuracy.

Table 3. UIUC Avistar UAV propulsion system component specifications.

Propulsion	
Motor	Model Motors AXI 4120/14 Outrunner
ESC	Castle Creation Phoenix Edge 75 Amp Brushless Speed Controller
Propeller	Landing Products APC 13x8E
Motor Flight Pack	Thunder Power ProLiteX 25c 4S 14.8 V 6 Ah lithium polymer battery

Table 4. Al Volo FC+DAQ system component specifications as installed on the UIUC Avistar UAV

Data acquisition system	Al Volo FC+DAQ 400 Hz system
Sensors	
Inertial measurement unit	XSens MTi-G-710 AHRS with GPS
Airspeed sensor	Al Volo Pitot Static Airspeed Sensor
Motor sensor	Al Volo Castle ESC Interface
Power	
Regulator	Built into FC+DAQ
Battery	Thunder Power ProLiteX 25c 3S 11.1 V 1350 mAh lithium polymer battery

Figure 10. The integrated Hall-effect current sensor (circled in red) next to the ESC in the UIUC Avistar UAV; note that these components are situated on the battery tray with the firewall and nose of the aircraft to the right.

C. UIUC-TUM Solar Flyer

The UIUC-TUM Solar Flyer has the ultimate aim of sustaining continuous flight for extended periods of time while performing on-board, real-time computation and to shift the paradigm of solar powered flight. The traditional approach for small size UAVs, is to capture data on the aircraft, stream it to the ground through a high power data-link, process it remotely (potentially off-line), perform analysis, and then relay commands back to the aircraft as needed. However, given the finite energy resources found onboard an aircraft (e.g. batteries and solar arrays), the traditional design greatly limits aircraft endurance, since significant power is consumed for transmission of visual data instead of being allocated to keeping the aircraft flying. The UIUC Solar Flyer was developed to carry a high performance embedded computer system to minimize the need for data transmission. The process of reducing aircraft power consumption allows for

decreasing aircraft size, prolonging flight time, and ultimately minimizing cost, therefore supporting the widespread adoption of UAVs for various types of missions.

The UIUC-TUM Solar Flyer was built from a majority of COTS components using a mixture of trade studies and power simulations in order to enable a variety of all-daylight hour missions while minimizing aircraft size. The 4.0 m (157 in) wingspan aircraft weighs approximately 3.3 kg (7.2 lb). The airframe was constructed from a F5 Models Pulsar 4.0E Pro remote control aircraft sailplane kit.[54] The fuselage is composed of a kevlar pod and a carbon fiber tail boom. The wings are composed out of 3 sections: center with flaps and outer right and left with aileron. The airframe was built per the manufacturer instructions with slight modifications to ease computational device and solar array integration.

As mentioned above, the Solar Flyer propulsion system components were selected using a propulsion system optimization tool,[55] which was applied to a typical field coverage mission the aircraft would perform.[56] The tool used the propeller performance data for 40 Aero-Naut CAM carbon folding propellers and motor parameters for 28 motors from Hacker Motor GmbH,[57] Model Motors s. r. o.,[58] and Neutronics,[59] which were mass and size compatible to the aircraft. 1120 combinations were computed and ranked by the efficiency. After considering thrust requirements for upset scenarios and thermal management, the Model Motors AXi 480/1380 and Aero-Naut CAM 12x8 were chosen as this combination provided a 15% increase in propulsion efficiency than the baseline combination and ample aircraft safety. Finally, in order to control and power the motor, a Castle Creations Phoenix Edge Lite 50A electronic speed controller (ESC) was chosen as it provided sufficient current capability and the required interfaces and sensing.

The aircraft energy storage systems were developed to collect, store, and distribute energy on-board as required. Gallium arsenide (GaAs) solar arrays from Alta Devices, which are estimated to be 25–26% efficient, are used on the aircraft in conjunction with a maximum power point tracking (MPPT) charge controller and a 3S 8P, 10.8V 28Ah Samsung 35E 18650 lithium-ion battery that acts as an energy buffer. The aircraft carries 64 W of solar cells mounted onto the upper surface of the wings; areas such as the leading edge and the control surfaces do not have solar cells mounted on them due to overhead weight and wiring associated as well as the decreased solar power production potential. The batteries are distributed within the fuselage, while maintaining center of gravity location. A side view of the fuselage layout is shown in Fig. 11. The specifications of the propulsion, energy storage, and solar systems is given in Table 5.

The UIUC-TUM Solar Flyer avionics are based around a commercially available flight control and data acquisition system, the Al Volo FC+DAQ, and uses the open-source uavAP autopilot[12,60] and uavGS ground station interface.[42,61] The system integrates a 9-DOF inertial measurement unit (IMU) and 10 Hz Global Navigation Satellite System (GNSS) and operates at 100 Hz. The main avionics unit as well as the airspeed probe and sensor, GNSS antenna, ESC data interface, 900 MHz radio module, and control multiplexer are laid out within the center wing panel; a top view of the instrumentation layout within the wing is shown in Fig. 12. Specifications of the avionics is provided in Table 6. Further detail regarding the UIUC-TUM Solar Flyer avionics development, and layout can be found in related literature.[44]

Table 5. UIUC-TUM Solar Flyer propulsion, energy storage, and solar systems specifications.

Propulsion	
Motor	Model Motors AXi Cyclone 46/760
ESC	Castle Creations Phoenix Edge Lite 50
Propeller	Aeronaut CAM Folding 13x6.5
Energy Storage	
Battery	10.8V 28Ah Samsung 35E 18650 in 3S 8P
Solar	
Photo Voltaic Cells	64W of Alta Devices Single Junction GaAS cells in 20S, 16P
Blocking & Bypass Diodes	80x Diodes Inc. 12A SBR
Charge Controller	Analog Devices MPPTs in 3P
Current Tracking	Allegro Hall-Effect Current Sensor

Table 6. Al Volo FC+DAQ system component specifications as installed on the UIUC-TUM Solar Flyer.

Autopilot-DAQ system	Al Volo FC+DAQ 100 Hz flight control and data acquisition system
RF Module	Digi International 900 MHz XBee Pro S3B Module
Multiplexer	8-channel PWM multiplexer with redundant input
Sensors	
Inertial	100 Hz AHRS integrated into FC+DAQ
Positioning	10 Hz GNSS integrated into FC+DAQ
Airspeed sensor	Al Volo Pitot Static Airspeed Sensor
Motor sensor	Al Volo Castle ESC Interface
Power Regulator	Built into FC+DAQ

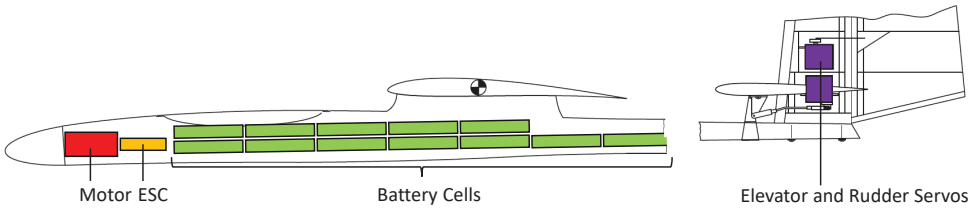

Figure 11. Side view of the UIUC-TUM Solar Flyer fuselage, showing the layout of the motor, the ESC, the battery cells, and the elevator and rudder servos.

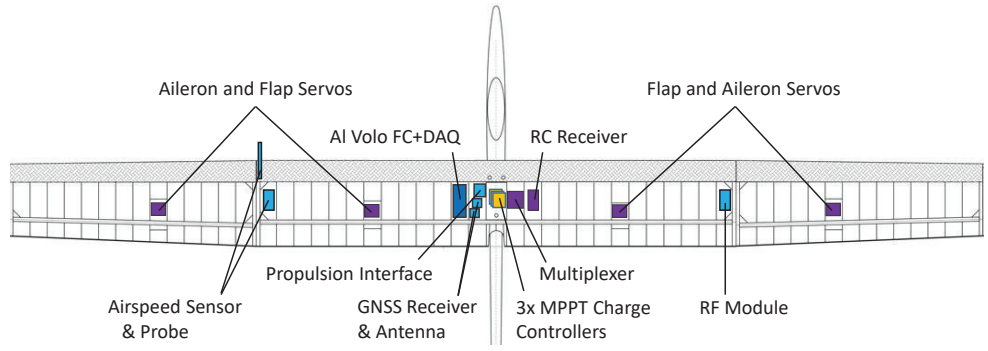

Figure 12. Top view of the UIUC-TUM Solar Flyer center and mid-outer wing sections, showing the layout of avionics components, MPPTs, and the aileron and flap servos.

The UIUC-TUM Solar Flyer uses both both direct input sensing and direct and in-direct output sensing to monitor aircraft power. Figure 13 presents a system-level power diagram of the systems on the UIUC-TUM Solar Flyer. Input sensing of the solar arrays (P_{array}) consists of 3 sets of power sensors which are located with the MPPT charge controllerss; these sensors are assembled from analog-to-digital convertor (ADC) voltage sensors and hall-effect current sensors. Power input (assumed positive) from the batteries consists of calculating the difference between the power output measurement (as measured by the propulsion power sensor ($P_{propulsion}$) and the avionics power sensor ($P_{avionics}$)) and the power input measurement from the arrays (P_{array}); the power bus is assumed to be transparent. The power output measurement is measured in several ways: (1) input power to the ESC via an analog-to-digital convertor (ADC) voltage sensors and hall-effect current sensors at $P_{propulsion}$, (2) output power from the ESC via a built-in information interface at P_{ESC}, and (3) output power from the motor and propeller via measurement of the propeller rotation rate using a motor-pulse tachometer, measurement of the aircraft freestream velocity using a pitot probe, and with knowledge of propeller performance. A key challenge in integrating this sensing into the UIUC-TUM Solar Flyer was placement about the aircraft.

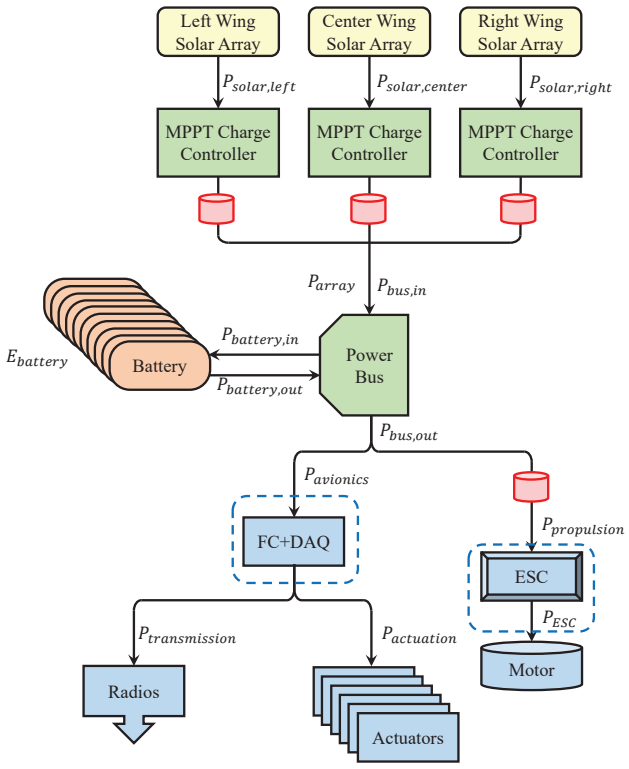

Figure 13. A system-level power diagram of the UIUC-TUM Solar Flyer, showing power input devices (yellow and orange), input modulating devices (green), power output/consuming devices (blue), and power measurement devices (red); note that the left set of power consuming devices (blue) are not part of the propulsion system but rather of flight control and instrumentation.

During the 2020 and 2021 flight seasons, the UIUC-TUM Solar Flyer performed several long-endurance, solar-powered flights, the longest of which was 9 hours under a mixture of ideal and non-ideal weather conditions (high wind and clouds). For the purposes of examining power monitoring, a 1 hour flight[62] performed under ideal conditions is presented. The approximately 1 hour flight was performed on Oct 8, 2020 with take off at 11:43 AM. During the flight, the sun shifted from 42 deg elevation and 158 deg azimuth to 45 deg elevation and 177 deg azimuth. At the field, the flight crew observed sunny skies with the winds of 3-5 mph (1.3-2.2 m/s) from the SSW (190-210 deg), which was aligned with the runway, from right to left (in the perspective of the flight crew).

The trajectory of the flight is shown in Fig. 14. The aircraft was commanded to perform a race track pattern of 650×150 m at an altitude of 100 m AGL; and maintain an airspeed of 11 m/s. The race track path flown is equivalent in flight maneuvering to an area coverage mission with 500 m long straights that are 150 m apart, with required 180 deg, 75 m radius turn-arounds at the ends of the straights. 26 laps were performed during the 53 min of maneuvering, yielding an effective coverage area of 1.95 km^2 (481 acre). Therefore, the race track maneuvering demonstrated equates to an area coverage of 2.2 km^2/hr (545 $acre/hr$).

The state data time history is presented in Fig. 19. The aircraft position and altitude are presented in (a) and (b), respectively. The Euler angle pitch and roll are presented in (c) and heading is presented in (d). The aircraft air and ground speeds are presented in (e); the ground speed is measured by the GNSS while airspeed is computed by a wind-tunnel calibrated airspeed sensor. The ESC and motor propulsion power, measured between the battery and ESC and between the ESC and motor, respectively, is presented in (f). The propeller rotation rate, measured by the ESC, is presented in RPM in (g). The battery voltage is presented in (h). The MPPT currents presented in (i). And the solar power generated by the solar arrays is presented in (j).

The position and Euler angle data shows 26 race track laps being performed, each approximately 2 min long. There are an increasing amount of mostly positive vertical excursions from the commanded altitude during the middle part of

the flight. The airspeed data shows an attempt to maintain the 11 m/s commanded airspeed with increased airspeeds correlating to the times when the positive vertical excursions occurred. There are also a repeated offsets between air and ground speed, which result from wind; the magnitude is either positive or negative based on whether the aircraft is flying upwind or downwind.

The propulsion power heavily oscillates during the flight for both the motor and ESC. There is a decrease in on-power times used during the middle of the flight when positive vertical excursions occurred; these are also the same times when the airspeed exceeded the commanded 11 m/s. It is assumed that the uncommanded positive altitude deviations are the result of thermals. During this time, the ESC throttles the motor off with the propeller wind milling. Meanwhile, the negative altitude deviations seem to be the result of an interplay between the autopilot attempting to pitch the aircraft downward to maintain altitude and often, the thermals weakening. As a result, the ESC is commanded to throttle-up the motor to create thrust and increase airspeed, which corresponds to propulsion power consumption.

Thus, the throttling-on and throttling-off of the motor is the result of the interplay between the autopilot and ESC controllers and limits. With the earlier thermal assumption, it is assumed that some of the energy used to propel the aircraft and counter drag also comes from thermals through the uncommanded altitude and thus potential energy gains. In order to better estimate propulsion power consumption, 10 min moving averages of the race track laps were calculated, comprising of 5 laps of 60,000 data points each, yielding average power values between 14 and 53 W. As expected, the propeller rotation rate correlates with the propulsion power, i.e., when propulsion power is high, the propeller rotation rate increases to approximately 6,400 RPM, while when propulsion power is near 0, the propeller rotation rate decreases to approximately 2,900 RPM. This is indicative of the ESC throttling the motor on when the airspeed dips below 11 m/s and then off when it is above that airspeed.

During the flight the MPPT currents are seen oscillating with aircraft orientation as it flies about the race track trajectory. The left MPPT seems to be better oriented when it faces towards the sun during the right to left straight leg compared to the right MPPT when when it faces towards the sun during the left to right straight leg. The center MPPT has less solar cells in its array, 80 cells as opposed to 120 cells for the left and right MPPTs, and therefore produces less current throughout the flight. Finally, the solar power is observed to vary cyclically between 14 and 55 W, correlating to the aforementioned repeated re-orientation of the aircraft as laps are being performed. Over the entire flight, the average solar power was approximately 35 W. The results show that power consumption was balanced with power generation. This is supported by the fact that, with the exception of an oscillation during takeoff, the battery voltage remains constant at 12.05 V for the entire flight.

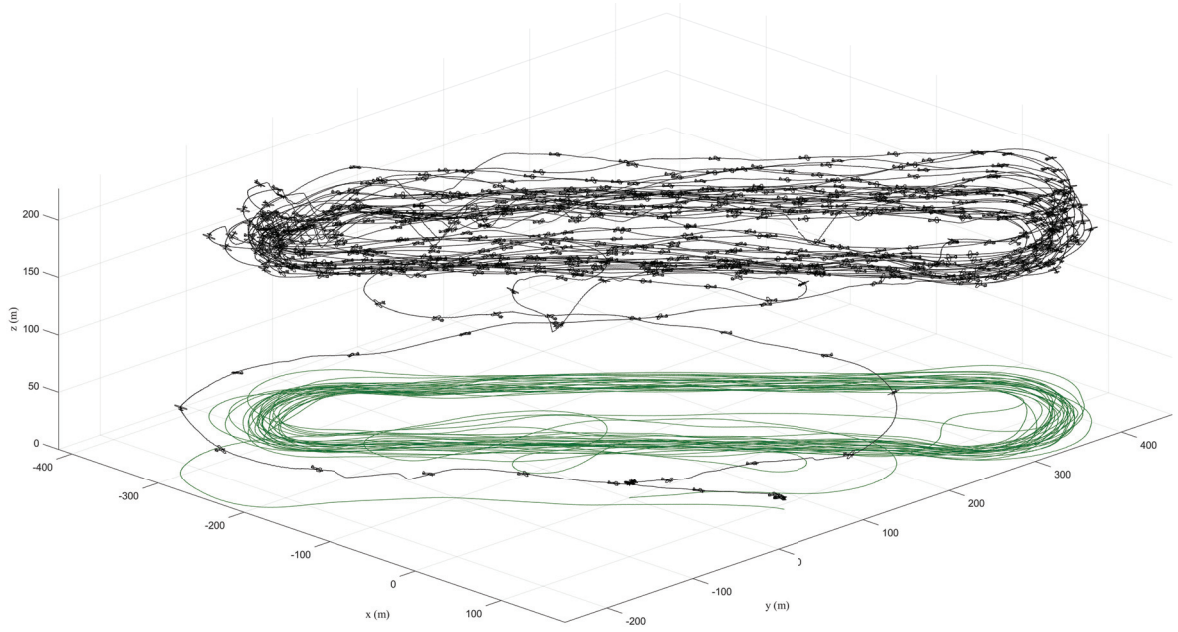

Figure 14. The trajectory of the UIUC-TUM Solar Flyer performing the approximately 1 hour flight under ideal conditions (note that the aircraft is plotted every 5 sec).

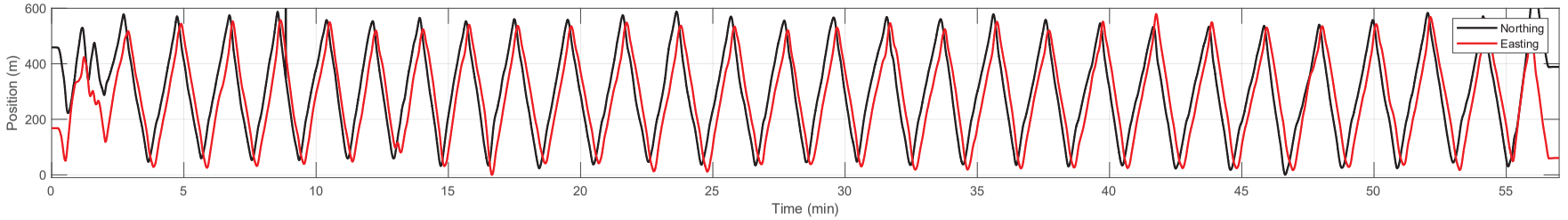

Figure 15.

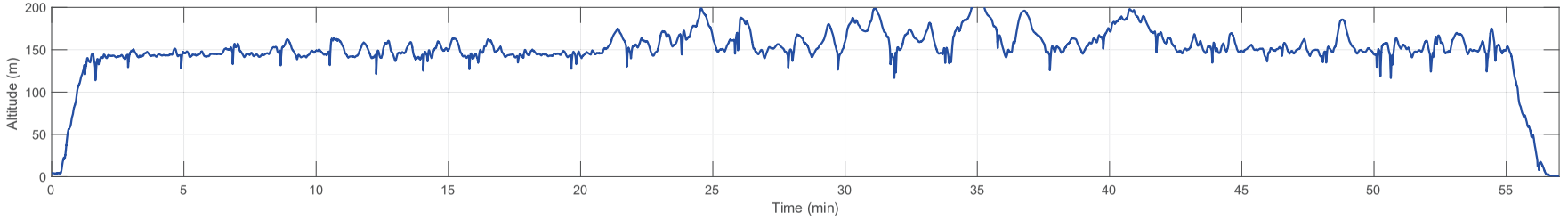

Figure 16.

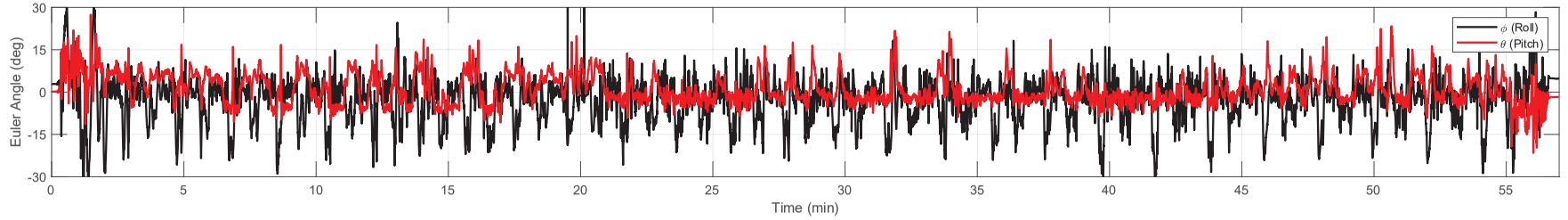

Figure 17.

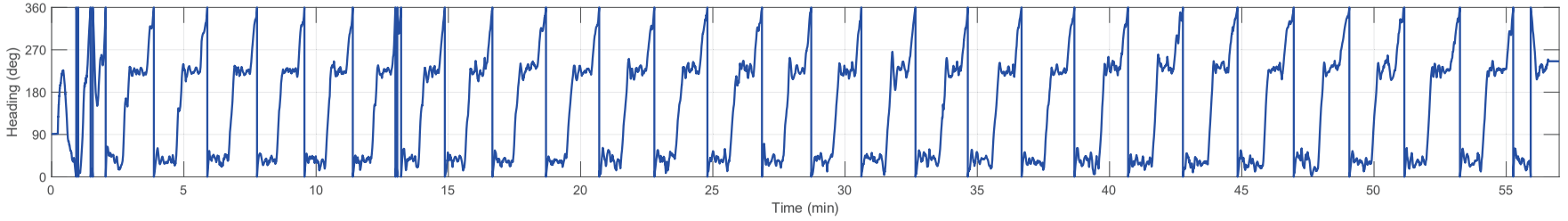

Figure 18

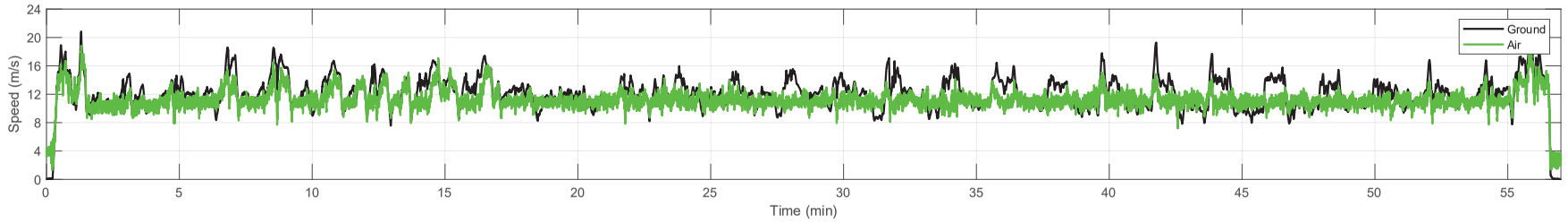

Figure 5 (continued).

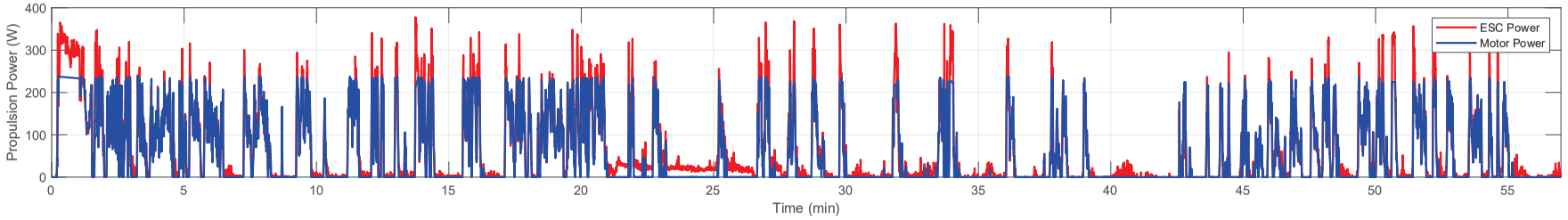

Figure 5 (continued).

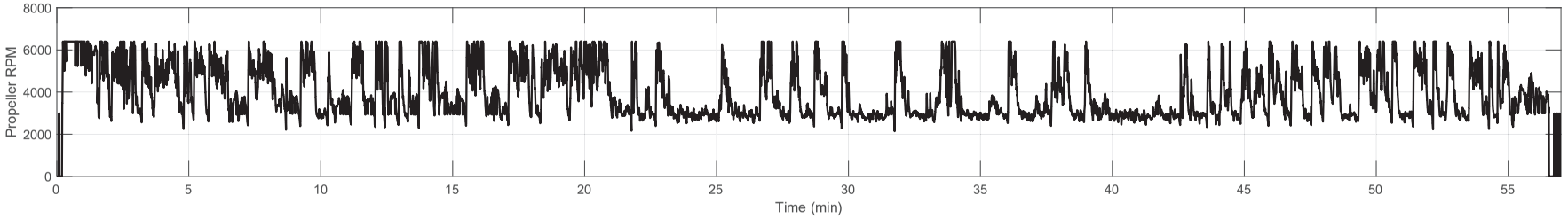

Figure 5 (continued).

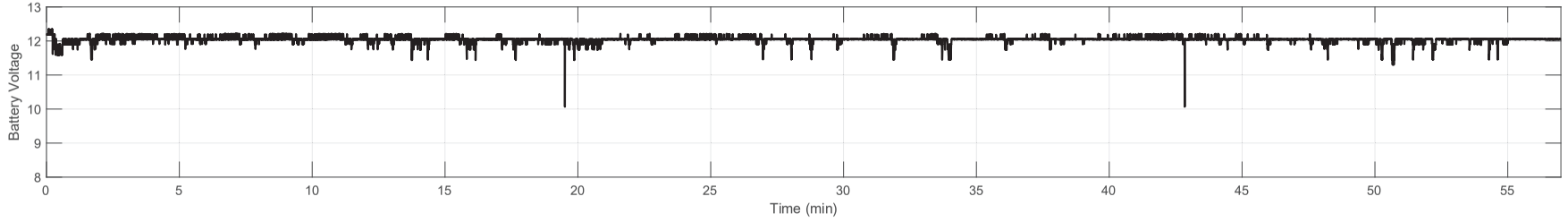

Figure 5 (continued).

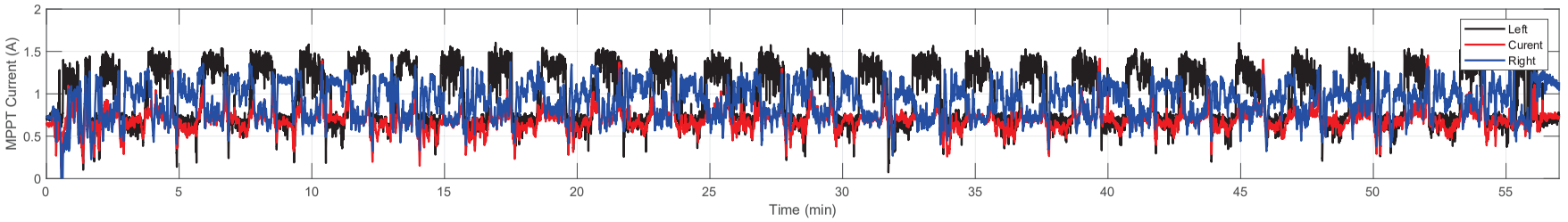

Figure 5 (continued).

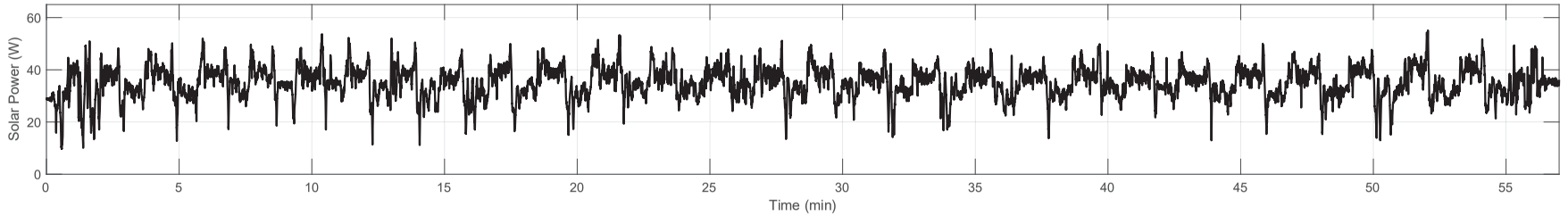

Figure 5 (continued).

Figure 5 (continued). The state data time history of the UIUC-TUM Solar Flyer performing the approximately 1 hour flight under ideal conditions: (i) MPPT current, (j) solar power generated.

V. Summary

This paper focused on the requirements, design, development, and integration to perform in-flight measurements of propulsion system parameters on small- and medium-sized electric unmanned aircraft. First, the paper provided an overview for the development of a data acquisition systems on unmanned aircraft followed by the instrumentation aspects involved in integrating propulsion system sensors and interfaces into existing system architectures. Then, the paper presented propulsion system sensing integration examples in different types of electric unmanned aircraft used for research. Flight data was presented for the last aircraft, demonstrating propulsion system data that can be gathered in-flight.

References

[1]Lykins, R. and Keshmiri, S., "Modal Analysis of 1/3-Scale Yak-54 Aircraft Through Simulation and Flight Testing," AIAA Paper 2011-6443, AIAA Atmospheric Flight Mechanics Conference, Portland, Oregon, Aug. 2011.

[2]Johnson, B. and Lind, R., "Characterizing Wing Rock with Variations in Size and Configuration of Vertical Tail," *Journal of Aircraft*, Vol. 47, No. 2, 2010, pp. 567–576.

[3]Dantsker, O. D., Yu, S., Vahora, M., and Caccamo, M., "Flight Testing Automation to Parameterize Unmanned Aircraft Dynamics," AIAA Paper 2019-3230, AIAA Aviation and Aeronautics Forum and Exposition, Dallas, TX, Jun. 2019.

[4]Perry, J., Mohamed, A., Johnson, B., and Lind, R., "Estimating Angle of Attack and Sideslip Under High Dynamics on Small UAVs," Proceedings of the ION-GNSS Conference, Savannah, Georgia, 2008.

[5]Uhlig, D., Sareen, A., Sukumar, P., Rao, A. H., and Selig, M. S., "Determining Aerodynamic Characteristics of a Micro Air Vehicle Using Motion Tracking," AIAA Paper 2010-8416, AIAA Guidance, Navigation, and Control Conference, Toronto, Ontario, Canada, Aug. 2010.

[6]Dantsker, O. D. and Selig, M. S., "High Angle of Attack Flight of a Subscale Aerobatic Aircraft," AIAA Paper 2015-2568, AIAA Applied Aerodynamics Conference, Dallas, Texas, Jun. 2015.

[7]Frank, A., McGrewy, J. S., Valentiz, M., Levinex, D., and How, J. P., "Hover, Transition, and Level Flight Control Design for a Single-Propeller Indoor Airplane," AIAA Paper 2007-6318, AIAA Guidance, Navigation, and Control Conference, Hilton Head, South Carolina, Aug. 2007.

[8]Johnson, E. N., Wu, A. D., Neidhoefer, J. C., Kannan, S. K., and Turbe, M. A., "Test Results of Autonomous Airplane Transitions Between Steady-Level and Hovering Flight," *Journal of Guidance, Control, and Dynamics*, Vol. 31, No. 2, 2008, pp. 358–370.

[9]Bilodeau, P. R., Poulin, E., Gagnon, E., Wong, F., and Desbiens, A., "Control of a Hovering Mini Fixed Wing Aerial Vehicle," AIAA Paper 2009-5794, AIAA Guidance, Navigation and Control Conference, Chicago, Illinois, Aug. 2009.

[10]Johnson, B. and Lind, R., "Trajectory Planning for Sensing Effectiveness with High Angle-of-Attack Flight Capability," AIAA Paper 2012-0276, AIAA Aerospace Sciences Meeting, Nashville, Tennessee, Jan. 2012.

[11]Koch, W., Mancuso, R., West, R., and Bestavros, A., "Reinforcement learning for UAV attitude control," *ACM Transactions on Cyber-Physical Systems*, Vol. 3, No. 2, 2019, pp. 1–21.

[12]Theile, M., Dantsker, O. D., Caccamo, M., and Yu, S., "uavAP: A Modular Autopilot Framework for UAVs," AIAA Paper 2020-3268, AIAA Aviation 2020 Forum, Virtual Event, Jun. 2020.

[13]Jordan, T. L. and Bailey, R. M., "NASA Langley's AirSTAR Testbed: A Subscale Flight Test Capability for Flight Dynamics and Control System Experiments," AIAA Paper 2008-6660, AIAA Atmospheric Flight Mechanics Conference, Honolulu, HI, Aug. 2008.

[14]Ragheb, A. M., Dantsker, O. D., and Selig, M. S., "Stall/Spin Flight Testing with a Subscale Aerobatic Aircraft," AIAA Paper 2013-2806, AIAA Applied Aerodynamics Conference, San Diego, CA, June 2013.

[15]Bunge, R. A., Savino, F. M., and Kroo, I. M., "Approaches to Automatic Stall/Spin Detection Based on Small-Scale UAV Flight Testing," AIAA Paper 2015-2235, AIAA Atmospheric Flight Mechanics Conference, Dallas, Texas, Jun. 2015.

[16]Risch, T., Cosentino, G., Regan, C., Kisska, M., and Princen, N., "X-48B Flight-Test Progress Overview," AIAA Paper 2009-934, AIAA Aerospace Sciences Meeting, Orlando, FL, Jan. 2009.

[17]Lundstrom, D. and Amadori, K., "Raven: A Subscale Radio Controlled Business Jet Demonstrator," International Congress on the Aeronautical Sciences Systems (ICUAS), Anchorage, Alaska, Sep. 2008.

[18]Regan, C. D. and Taylor, B. R., "mAEWing1: Design, Build, Test - Invited," AIAA Paper 2016-1747, AIAA Atmospheric Flight Mechanics Conference, San Diego, California, Jun. 2016.

[19]Regan, C. D., "mAEWing2: Conceptual Design and System Test," AIAA Paper 2017-1391, AIAA Atmospheric Flight Mechanics Conference, Grapevine, Texas, Jun. 2017.

[20]Leong, H. I., Keshmiri, S., and Jager, R., "Evaluation of a COTS Autopilot and Avionics System for UAVs," AIAA Paper 2009-1963, AIAA Infotech@Aerospace, Seattle, Washington, April. 2009.

[21]Esposito, J. F. and Keshmiri, S., "Rapid Hardware Interfacing and Software Development for Embedded Devices Using Simulink," AIAA Paper 2010-3415, AIAA Infotech@Aerospace, Atlanta, Georgia, June 2010.

[22]Garcia, G. and Keshmiri, S., "Integrated Kalman Filter for a Flight Control System with Redundant Measurements," AIAA Paper 2012-2499, AIAA Infotech@Aerospace, Garden Grove, California, June 2012.

[23]Dantsker, O. D. and Mancuso, R., "Flight Data Acquisition Platform Development, Integration, and Operation on Small- to Medium-Sized Unmanned Aircraft," AIAA Paper 2019-1262, AIAA SciTech Forum, San Diego, California, Jan 2019.

[24]Dantsker, O. D., Theile, M., and Caccamo, M., "Integrated Power Modeling for a Solar-Powered, Computationally-Intensive Unmanned Aircraft," AIAA Paper 2020-3568, AIAA/IEEE Electric Aircraft Technology Symposium, Virtual Event, Aug. 2020.

[25]Drela, M., "First-Order DC Electric Motor Model," http://web.mit.edu/drela/Public/web/qprop/motor1$_theory.pdf$.

[26]Ol, M., Zeune, C., and Logan, M., "Analytical/Experimental Comparison for Small Electric Unmanned Air Vehicle Propellers," *26th AIAA Applied Aerodynamics Conference*, American Institute of Aeronautics and Astronautics, Reston, Virigina, 8 2008.

[27]Brandt, J., Deters, R., Ananda, G., Dantsker, O., and Selig, M., "UIUC Propeller Database," http://m-selig.ae.illinois.edu/props/propDB.html, Accessed Dec. 2021.

[28]Dantsker, O. D., Caccamo, M., Deters, R. W., and Selig, M. S., "Performance Testing of Aero-Naut CAM Folding Propellers," AIAA Paper 2020-2762, AIAA Aviation 2020 Forum, Virtual Event, Jun. 2020.

[29]McCrink, M. H. and Gregory, J. W., "Blade Element Momentum Modeling for Low-Re Small UAS Electric Propulsion Systems," AIAA Paper 2015-3191, AIAA Aviation Forum, Dallas, Texas, Jun. 2015.

[30]Dantsker, O. D., Ananda, G. K., and Selig, M. S., "GA-USTAR Phase 1: Development and Flight Testing of the Baseline Upset and Stall Research Aircraft," AIAA Paper 2017-4078, AIAA Applied Aerodynamics Conference, Denver, Colorado, June 2017.

[31]Bradt, J. B. and Selig, M. S., "Propeller Performance Data at Low Reynolds Numbers," *AIAA Aerospace Sciences Meeting, Orlando, Florida, Jan. 2011*.

[32]Deters, R. W. and Selig, M. S., "Static Testing of Micro Propellers," AIAA Paper 2008-6246, AIAA Applied Aerodynamics Conference, Honolulu, Hawaii, Aug. 2008.

[33]Deters, R. W., Dantsker, O. D., Kleinke, S., Norman, N., and Selig, M. S., "Static Performance Results of Propellers Used on Nano, Micro, and Mini Quadrotors," AIAA Paper 2018-4122, AIAA Aviation Forum, Atlanta, Georgia, June 2018.

[34]Dantsker, O. D., Deters, R. W., and Caccamo, M., "Propulsion System Testing for a Long-Endurance Solar-Powered Unmanned Aircraft," AIAA Paper 2019-3688, AIAA Applied Aerodynamics Conference, Dallas, TX, Jun. 2019.

[35]"Adafruit Industries," https://www.adafruit.com/.

[36]"Sparkfun Electronics," https://www.sparkfun.com/.

[37]"Cytron Technologies," https://www.cytron.io/.

[38]"Phidgets Inc." https://www.phidgets.com/.

[39]Castle Creations, Inc., http://castlecreations.com/.

[40]Dantsker, O. D., Loius, A. V., Mancuso, R., Caccamo, M., and Selig, M. S., "SDAC-UAS: A Sensor Data Acquisition Unmanned Aerial System for Flight Control and Aerodynamic Data Collection," *AIAA Paper 2015-0987, AIAA Infotech@Aerospace Conference, Kissimee, Florida, Jan 2015.*.

[41]Dantsker, O. D., Theile, M., and Caccamo, M., "A High-Fidelity, Low-Order Propulsion Power Model for Fixed-Wing Electric Unmanned Aircraft," AIAA/IEEE Electric Aircraft Technologies Symposium, Jul. 2018.

[42]Theile, M., Dantsker, O. D., Nai, R., and Caccamo, M., "uavEE: A Modular, Power-Aware Emulation Environment for Rapid Prototyping and Testing of UAVs," Accepted to IEEE International Conference on Embedded and Real-Time Computing Systems and Applications, Hakodate, Japan, Aug. 2018.

[43]Dantsker, O. D., Theile, M., Caccamo, M., and Mancuso, R., "Design Development and Initial Testing of a Computationally-Intensive Long-Endurance Solar-Powered Unmanned Aircraft," AIAA Paper 2018-4217, AIAA Applied Aerodynamics Conference, Atlanta, Georgia, June 2018.

[44]Dantsker, O. D., Theile, M., Caccamo, M., Yu, S., Vahora, M., and Mancuso, R., "Continued Development and Flight Testing of a Long-Endurance Solar-Powered Unmanned Aircraft: UIUC-TUM Solar Flyer," AIAA Paper 2020-0781, AIAA Scitech 2020 Forum, Orlando, FL, Jan. 2020.

[45]Real Time and Embedded System Laboratory, University of Illinois at Urbana-Champaign, "Solar-Powered Long-Endurance UAV for Real-Time Onboard Data Processing," http://rtsl-edge.cs.illinois.edu/UAV/.

[46]Mancuso, R., Dantsker, O. D., Caccamo, M., and Selig, M. S., "A Low-Power Architecture for High Frequency Sensor Acquisition in Many-DOF UAVs," International Conference on Cyber-Physical Systems, Berlin, Germany, Apr. 2014.

[47]Dantsker, O. D., Mancuso, R., Selig, M. S., and Caccamo, M., "High-Frequency Sensor Data Acquisition System (SDAC) for Flight Control and Aerodynamic Data Collection Research on Small to Mid-Sized UAVs," AIAA Paper 2014-2565, AIAA Applied Aerodynamics Conference, Atlanta, Georgia, June 2014.

[48]Al Volo LLC, "Al Volo: Flight Data Acquisition Systems," http://www.alvolo.us.

[49]Dantsker, O. D., Selig, M. S., and Mancuso, R., "A Rolling Rig for Propeller Performance Testing," AIAA Paper 2017-3745, AIAA Applied Aerodynamics Conference, Denver, Colorado, Jun. 2017.

[50]Dantsker, O. D., Vahora, M., Imtiaz, S., and Caccamo, M., "High Fidelity Moment of Inertia Testing of Unmanned Aircraft," AIAA Paper 2018-4219, AIAA Aviation and Aeronautics Forum and Exposition, Atlanta, Georgia, Jun. 2018.

[51]Dantsker, O. D., Theile, M., and Caccamo, M., "A High-Fidelity, Low-Order Propulsion Power Model for Fixed-Wing Electric Unmanned Aircraft," AIAA Paper 2018-5009, AIAA/IEEE Electric Aircraft Technologies Symposium, Cincinnati, OH, Jul. 2018.

[52]Dantsker, O. D., Caccamo, M., Vahora, M., and Mancuso, R., "Flight & Ground Testing Data Set for an Unmanned Aircraft: Great Planes Avistar Elite," AIAA Paper 2020-0780, AIAA SciTech Forum, Orlando, Florida, Jan 2020.

[53]Xsens Technologies B.V., "Xsens 3D motion tracking," http://www.xsens.com/.

[54]"F5 Models," http://f5models.com, Accessed Oct. 2017.

[55]Dantsker, O. D., Imtiaz, S., and Caccamo, M., "Electric Propulsion System Optimization for a Long-Endurance and Solar-Powered Unmanned Aircraft," AIAA Paper 2019-4486, AIAA/IEEE Electric Aircraft Technology Symposium, Indianapolis, Indiana, Aug. 2019.

[56]Dantsker, O. D., Imtiaz, S., and Caccamo, M., "Propulsion System Design, Optimization, Simulation, and Testing for a Long-Endurance Solar-Powered Unmanned Aircraft," AIAA Propulsion and Energy Forum 2020, Virtual Event, Aug. 2020.

[57]Hacker Motor GmbH, "Hacker Brushless Motors," https://www.hacker-motor.com/, Accessed Aug. 2020.

[58]Model motors s.r.o., "AXI Model Motors," http://www.modelmotors.cz/, Accessed Jun. 2021.

[59]Neutronics, "NeuMotors," https://neumotors.com/, Accessed Aug. 2020.

[60]M. Theile, "uavAP: A Modular Autopilot for Unmanned Aerial Vehicles," https://github.com/theilem/uavAP, Accessed Mar. 2021.

[61]Mirco Theile, "uavGS: A Modular Ground Station Interface for Unmanned Aerial Vehicles," https://github.com/theilem/uavGS.

[62]Dantsker, O. D., Theile, M., and Caccamo, M., "Long Endurance Flight Testing Results for the UIUC-TUM Solar Flyer," AIAA Paper 2021-3196, AIAA Aviation Forum, Virtual Event, Aug. 2021.

View publication stats